Imaging the interaction of HIV-1 genomes and Gag during assembly of individual viral particles

Nolwenn Jouvenet[a], Sanford M. Simon[b,1], and Paul D. Bieniasz[a,c,2]

[a]Aaron Diamond AIDS Research Center and [b]Laboratory of Cellular Biophysics, The Rockefeller University, New York, NY 10065; and [c]The Howard Hughes Medical Institute, New York, NY 10016

Edited by John M. Coffin, Tufts University School of Medicine, Boston, MA, and approved September 11, 2009 (received for review July 1, 2009)

The incorporation of viral genomes into particles has never previously been imaged in live infected cells. Thus, for many viruses it is unknown how the recruitment and packaging of genomes into virions is temporally and spatially related to particle assembly. Here, we devised approaches to simultaneously image HIV-1 genomes, as well as the major HIV-1 structural protein, Gag, to reveal their dynamics and functional interactions during the assembly of individual viral particles. In the absence of Gag, HIV-1 RNA was highly dynamic, moving in and out of the proximity of the plasma membrane. Conversely, in the presence of Gag, RNA molecules docked at the membrane where their lateral movement slowed and then ceased as Gag assembled around them and they became irreversibly anchored. Viral genomes were not retained at the membrane when their packaging signals were mutated, nor when expressed with a Gag mutant that was not myristoylated. In the presence of a Gag mutant that retained membrane- and RNA-binding activities but could not assemble into particles, the viral RNA docked at the membrane but continued to drift laterally and then often dissociated from the membrane. These results, which provide visualization of the recruitment and packaging of genomes into individual virus particles, demonstrate that a small number of Gag molecules recruit viral genomes to the plasma membrane where they nucleate the assembly of complete virions.

RNA packaging | virion morphogenesis

HIV-1 Gag is the major viral structural protein, and its expression alone in many mammalian cells is sufficient to drive assembly of virus-like-particles (VLPs). Gag carries four distinct domains, each of which is required in the context of a single polypeptide during assembly (1, 2): an amino terminal matrix (MA) domain directs membrane binding, a central capsid (CA) domain provides protein-protein contacts for assembly and determines particle morphology, a nucleocapsid (NC) domain drives multimerization and packages two copies of the unspliced RNA genome (3), and a C-terminal p6 region recruits cellular factors necessary for the pinching off and release of nascent viral particles from the host cell membrane (1, 2).

Selection of viral genomes is mediated by interaction between the NC domain of Gag and a 120-nt segment of the viral genome called the Ψ sequence. The Ψ sequence comprises four closely spaced stem loops (SL-1 through SL-4) located within the 5′-untranslated region and the extreme 5′ end of the *gag* gene (4–7). Viral RNA dimerization and packaging may be coupled, since SL-1 also contains RNA sequences that initiate dimerization (8, 9). The major 5′ splice donor, required for the generation of spliced viral transcripts that encode accessory and envelope proteins, is found within SL-2. This location ensures that the packaging elements are disrupted upon splicing, providing a mechanism for discrimination between full-length genomes and spliced viral mRNAs. Indeed, the selective recruitment of the viral genome in a background of more abundant cellular RNA and spliced HIV-1 RNA is, at least in part, the result of the high affinity binding of SL-2 and SL-3 by NC (10, 11). Nonetheless, in the absence of the viral RNA, cellular RNAs are packaged (12, 13). This observation, and the finding that nucleic acid greatly stimulates the assembly of Gag into particles in vitro (14), suggests that viral or cellular RNA may nucleate the assembly of HIV-1 particles in cells.

The productive site of HIV-1 assembly is the plasma membrane, both in cultured cell lines and primary cells (15–17). This makes the assembly of HIV-1 accessible to imaging with total-internal-reflection (TIR) fluorescent microscopy, which selectively excites fluorophores in close proximity (≈<70 nm) to the coverslip. This technique has a sufficient signal to noise ratio to allow quantification of the assembly of individual HIV-1 particles, from initiation of assembly to budding and release (18). Our previous analyses, based on imaging of the Gag protein, revealed that a typical HIV-1 particle requires 5–6 min to complete assembly. However, the location and timing of the recruitment of other virion components, such as the viral genome, to nascent particles is unknown.

In this study, we devised a technique to visualize the recruitment of the HIV-1 genome to individual assembling particles. Simultaneous imaging of fluorescently tagged viral Gag protein and genomic RNA during particle assembly in live cells revealed that a few Gag molecules are required to recruit the viral RNA to the plasma membrane. The viral RNA arrives at the plasma membrane in a single step, suggesting that RNA dimers form before recruitment. Thereafter, this viral RNA:Gag subvirion complex recruits additional Gag molecules that are required to irreversibly anchor the viral RNA at the plasma membrane and nucleates the assembly of a complete virion particle.

Results

Labeling HIV-1 Genomes with GFP. To visualize the incorporation of HIV-1 genomes into virions, we fluorescently tagged both HIV-1 Gag and genomic RNA. Gag was expressed as a fusion to the fluorescent protein mCherry and co-expressed with WT Gag, which leads to the production of fluorescent VLPs with correct morphology (18). The HIV-1 RNA was tagged with stem loops that bind with high affinity and specificity to the coat protein of the bacteriophage MS2 (19, 20), which was expressed as a fusion protein to GFP. The tagged viral genome was derived from V1B (21), a modified HIV-1 proviral plasmid that expresses an RNA encoding a truncated version of the *gag* gene, all necessary *cis*-acting signals, such as the packaging (Ψ) sequence and the Rev response element, as well as the full-length *tat*, *rev*, and *vpu* genes. We inserted 24 copies of the MS2 RNA stem loop at the 3′ end of the truncated *gag* gene to create V1B-MS2 (Fig.

Author contributions: N.J., S.M.S., and P.D.B. designed research; N.J. performed research; N.J., S.M.S., and P.D.B. analyzed data; and N.J., S.M.S., and P.D.B. wrote the paper.

The authors declare no conflict of interest.

This article is a PNAS Direct Submission.

[1]To whom correspondence may be addressed at: Laboratory of Cellular Biophysics, The Rockefeller University, 1230 York Avenue, New York, NY 10065. E-mail: simon@mail.rockefeller.edu.

[2]To whom correspondence may be addressed at: Aaron Diamond AIDS Research Center, 455 First Avenue, New York NY, 10016 USA. E-mail: pbienias@adarc.org.

This article contains supporting information online at www.pnas.org/cgi/content/full/0907364106/DCSupplemental.

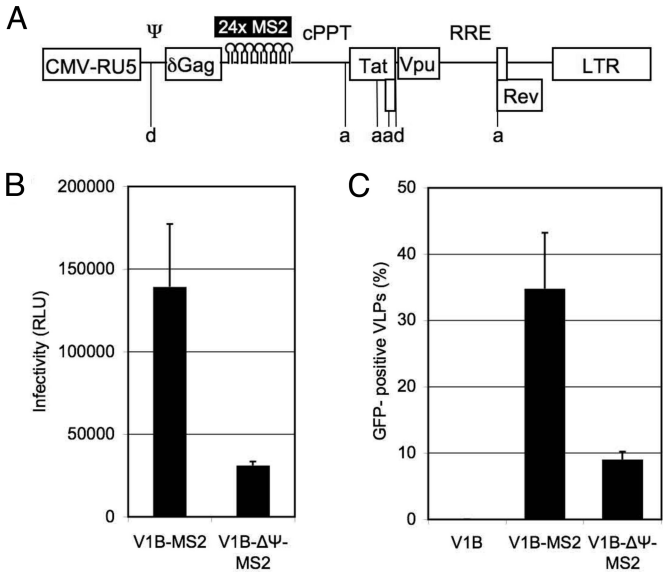

Fig. 1. HIV-1 genomes carrying MS2 binding sites are packaged and infectious. (*A*) Schematic of the MS2-tagged HIV-1 genome, V1B-MS2, used in these studies. The positions of critical *cis*-acting sequences, including packaging sequence (Ψ), the central polypurine tract (cPPT), and the Rev response element (RRE) are indicated, as are the positions of the salient splice donors (d) and acceptors (a). (*B*) Infectivity of virions generated by 293T cells coexpressing HIV-1 Gag-Pol, VSV-G envelope, and V1B-MS2 or V1B-ΔΨ-MS2 constructs. β-galactosidase activity following infection of TZM indicator cells was measured and plotted as the mean± SD relative light units (RLU). (*C*) The mean percentage ± SD of mCherry-VLPs that contained GFP-labeled genomes for V1B, V1B-MS2, or V1B-ΔΨ-MS2 (cumulative $n > 1000$ VLPs, three independent experiments).

1*A*). This ensured that only the unspliced, full-length genomic RNA would be tagged with MS2-GFP.

The ability of this modified viral RNA to generate infectious virions was tested using viral particles produced by 293T cells expressing HIV-1 Gag-Pol, the VSV-G envelope protein, and either V1B or V1B-MS2 RNA. Virions carrying the V1B-MS2 RNA genome were infectious, albeit approximately 10-fold less so than virions carrying the unmodified V1B genome (Fig. S1). This was not unexpected, as the insertion of the 24 stem loops into the viral RNA could affect the efficiency of reverse transcription. Nonetheless, the fact that virions generated in the presence of V1B-MS2 RNA were infectious confirmed that MS2-tagged viral genomes were packaged.

The specificity of RNA recruitment was tested with an MS2 stem-loop-containing viral genome truncated in the Ψ packaging sequence (V1B-ΔΨ-MS2). Since the V1B-MS2 genome also expresses the Rev protein, which is required for export of unspliced HIV-1 RNA (22), it was essential not to disrupt the 5′ splice donor site that is present in SL-2 of the Ψ sequence. Therefore, a segment of Ψ that encompasses SL-3 and SL-4, was deleted to generate V1B-ΔΨ-MS2. This deletion should reduce, but not completely abrogate packaging (10, 23), and Tat, Rev, and Vpu expression should be maintained. The virions generated using V1B-ΔΨ-MS2 were 4- to 5-fold less infectious than those generated using V1B-MS2 (Fig. 1*B*), suggesting that V1B-MS2 infectivity was dependent on Ψ integrity.

We generated a stable HeLa cell line expressing low, homogenous levels of MS2-GFP with a nuclear localization signal, (MS2-NLS-GFP). Thus, nascent HIV-1 transcripts could bind MS2-NLS-GFP in the nucleus, and the labeled RNA would be exported thereafter into the cytoplasm and packaged into virion particles. Each RNA molecule could carry a maximum of 48 copies of MS2-NLS-GFP (MS2 binds to the stem loops as dimer (24) and there are 24 MS2 stem loops per viral RNA molecule). However, this number is variable because not all of the 24 stem loops are always occupied by MS2 (19).

To test if GFP labeled RNA was incorporated in virions, we used TIR-FM to image VLPs collected from the supernatant of cells stably expressing MS2-NLS-GFP, and transiently transfected with V1B-MS2, Gag and Gag-mCherry (Fig. S2). Approximately one third of the Gag-mCherry VLPs (33%, n = 1,026) were positive for GFP (Fig. 1*C*). No VLPs had detectable GFP when the viral genome lacked the MS2 stem-loops and fewer than 10% (n = 1,043) had detectable GFP when the viral genome had a partial deletion in the packaging signal (V1B-ΔΨ-MS2) (Fig. 1*C* and Fig. S2). The quantitative deficit in GFP-labeled V1B-ΔΨ-MS2 RNA packaging was similar to the reduction in infectivity associated with Ψ truncation (Fig. 1 *B* and *C*) and, thus, GFP-labeled viral genome packaging was dependent on Ψ integrity.

The observation that only one-third of the VLPs contained GFP-labeled RNA may be due to a number of factors. First, Gag and the viral RNA were transiently expressed from separate plasmids, with transfected cells expressing variable levels of each plasmid. Supernatant samples contain VLPs generated by all cells, including cells that expressed low or undetectable levels of the viral genome. Consistent with this explanation, when we imaged the formation of VLPs on the surface of cells expressing both Gag-mCherry and V1B-MS2, 75% of the VLPs were positive for GFP-labeled RNA (see below). A second factor that could affect the incorporation of GFP-labeled RNA into VLPs is the kinetics of appearance of viral RNA and Gag in the cytosol. The Gag protein was expressed using a codon-optimized, Rev-independent expression vector. In contrast, export of the genomic HIV-1 RNA from the nucleus required that the HIV-1 RNA must first be spliced, exported from the nucleus, and then Rev translated and imported into the nucleus before the genomic RNA can be exported. Thus, in some cells, Gag appeared in the cytosol before the export of RNA. This would lead to the production of population of VLPs lacking the HIV-1 genome at early times after transfection. Nonetheless, these observations demonstrated that the fluorescently tagged viral genome can be assembled into VLPs.

Imaging HIV-1 Genomic RNA in Living Cells. In cells stably expressing MS2-NLS-GFP, the fluorescence was spread diffusely throughout the nucleus (Fig. 2*A*). In contrast, when these cells expressed the V1B-MS2 viral genome, the GFP fluorescence appeared as discrete spots in both the nucleus and cytoplasm (Fig. 2*B*). These MS2-GFP-bound RNA molecules were imaged at the basal surface of live cells using TIR fluorescence microscopy. Under our experimental configuration, the excitation falls exponentially to 1/e in 59 nm from the coverslip, limiting fluorescence to the immediate proximity of the plasma membrane. The puncta of GFP fluorescence moved in and out the field, remaining there for no more than few seconds (mean residence time = 3.64 s, n = 25) (Fig. 2*C* and Movie S1). There was no indication that the rapid movements were directed or confined either in the plane of the membrane or perpendicular to the membrane (Fig. 2*C*).

When cells that were transfected with V1B-MS2 also expressed HIV-1 Gag and Gag-mCherry, a subpopulation of GFP-labeled HIV-1 genomes colocalized with the mCherry labeled nascent VLPs at the cell surface, as observed by epifluorescence microscopy in fixed cells (Fig. S3*A*) or TIR-FM (Fig. S3*B*, upper panels). Early after transfection (4–6 h), some of the cells (60%) contained GFP-labeled RNA localized in the nucleus and Gag puncta at the plasma membrane (Fig. S4). This suggests that the Rev protein had yet to accumulate to sufficient levels to mediate efficient viral genome export in these cells. However, in the remaining cells (40%), in which both the Gag-mCherry protein and GFP-labeled viral genomes were

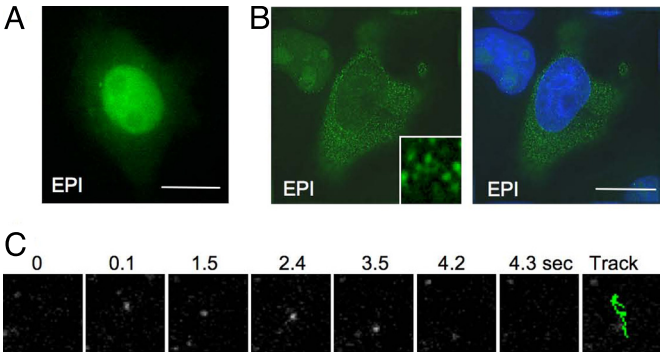

Fig. 2. Visualization of individual HIV-1 genomes in live HeLa cells. (*A*) MS2-NLS-GFP localizes primarily in the nucleus in the absence of HIV-1 genomes as imaged in epifluorescence (EPI) illumination. (Scale bar, 10 μm.) (*B*) Cells stably expressing MS2-NLS-GFP were transfected with V1B-MS2, fixed 24 h later. A deconvolved optical section from the center of the vertical dimension of the cell is shown. (Scale bar, 10 μm.) The inset shows an expanded segment of the image. The right panel shows the same image with nuclei revealed by staining with Hoechst 33258. (*C*) Cells stably expressing MS2-NLS-GFP were observed under TIR-FM 6 h after transfection with V1B-MS2. An RNA punctum was tracked and the numbers indicate the elapsed time (in seconds). Images are 5 × 5 μm. Far right image shows the track (green) of the RNA punctum.

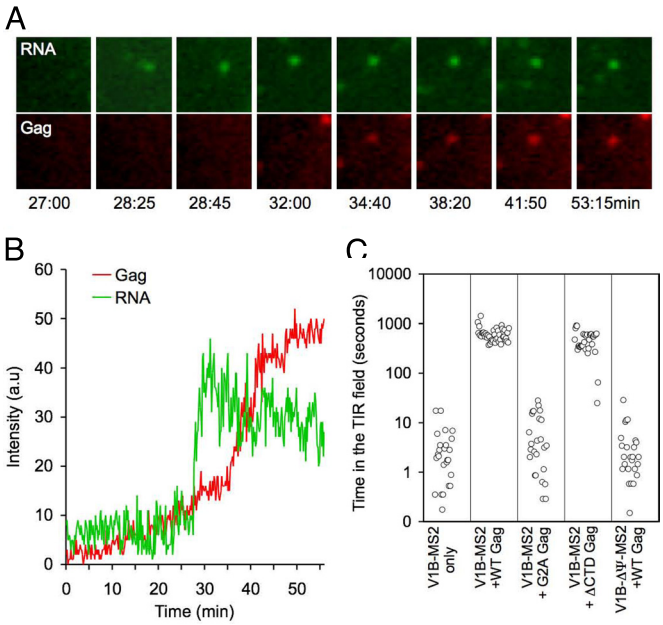

Fig. 3. Retention of viral RNA at the plasma membrane and VLP assembly on RNA. (*A* and *B*) Cells stably expressing MS2-NLS-GFP were transfected with Gag/Gag-mCherry and V1B-MS2 and observed live under TIR-FM beginning at 6 h post-transfection. (*A*) Images of an appearing GFP-labeled RNA punctum on which a VLP subsequently assembles. Images are 2.5 × 2.5 μm. Elapsed time is in minutes:seconds. (*B*) Plots of fluorescence intensity in arbitrary units (a.u) for the GFP-labeled RNA and Gag-mCherry signals for the VLP shown in (*A*). (*C*) Time for which GFP-labeled HIV-1 genomes remain in the TIR field. Each point represents an individual GFP-labeled RNA punctum, and the total time of residence in the TIR field is plotted. However, for ''V1B-MS2 + WT Gag'' only RNAs on which a VLP assembled are indicated, and the time taken from the appearance of the RNA to completion of the corresponding VLP assembly is plotted. For ''V1B-MS2 + Gag-ΔCTD'' only RNAs that became anchored at the plasma membrane, but both appeared and disappeared during the period of observation are plotted.

detectable in the cytoplasm, most of the Gag-mCherry VLPs (75%, $n = 441$) present at the plasma membrane colocalized with a GFP-labeled RNA (Fig. S3*B*, upper panels). In the presence of a packaging-impaired V1B-ΔΨ-MS2 viral RNA, a similar proportion of cells had GFP labeled viral genomes present in the cytoplasm (Fig. S3*B*, lower panels). However, in this case, far fewer (7.34%, $n = 327$) of the Gag-mCherry VLPs colocalized with GFP-labeled viral genomes.

Dynamics of HIV-1 RNA Molecules at the Plasma Membrane of Cells During Virion Assembly. Since we could observe GFP-labeled HIV-1 genomes that were exported into the cytoplasm, associated with VLPs in Gag-mCherry expressing cells, and packaged into extracellular VLPs in a Ψ-dependent manner, we attempted to characterize the behavior of viral genomes during VLP assembly. When V1B-MS2 was coexpressed with Gag/Gag-mCherry in HeLa MS2-NLS-GFP-expressing cells and imaged using dual-color TIR-FM, we observed four different behaviors for the GFP-labeled RNA molecules. One population moved in and out of the TIR field, with a time course of seconds. They were indistinguishable from the GFP-labeled RNA molecules observed in the absence of Gag (Movie S2) and did not colocalize with detectable Gag puncta at any time. A second population remained static in the TIR field during the entire period of image acquisition and their fluorescence always co-localized with Gag puncta (Fig. S5 and Movie S3). A third population of RNA molecules moved slowly in the TIR field and initially did not co-localize with detectable Gag-mCherry puncta. However, after a few minutes the mCherry fluorescence increased as the RNA stopped moving (Fig. 3 *A* and *B* and Movies S4 and S5). A fourth population of RNA molecules was associated with Gag puncta, and both moved together, rapidly in and out the TIR field (Fig. S6 and Movie S6).

The first population of rapidly appearing and disappearing RNAs may represent viral genomes that have not yet engaged Gag. Alternatively, they may represent RNA molecules that have bound Gag molecules that have yet to engage the plasma membrane. This was the only behavior that was observed for cytoplasmic RNA molecules that were generated in the absence of Gag (Fig. 2 and 3*C*, column 1), suggesting that residence of the HIV-1 RNA at the plasma membrane requires engagement with membrane-bound Gag. To test this hypothesis, we imaged GFP-labeled viral genomes together with a mutant of Gag (G2A) that cannot be myristoylated, is unable to stably bind the plasma membrane (25, 26) and therefore cannot produce VLPs. The behavior of the RNA molecules in the presence of the G2A-Gag-mCherry was indistinguishable from their behavior in the absence of Gag, that is, they did not remain in the TIR field for more than few seconds (mean = 7.5 s, $n = 25$) (Fig. 3*C*, column 3, Fig. S7, and Movie S7). Thus, these data strongly suggest that the membrane anchoring by Gag is required to anchor viral RNA at the plasma membrane.

The second population of viral RNA molecules that were static at the plasma membrane are likely packaged in VLPs. We have previously shown that static VLPs on the cell surface that are no longer recruiting Gag, have completed assembly and some have separated from the cell (18). Nonetheless, they rarely move away, either because they remain associated with the cell surface (27) or because they are trapped in the small space (≈40 nm) between the cell and the coverslip. Similarly, the static fluorescent spots we observed here that contain both Gag and viral RNA and whose intensities were constant over many minutes, are likely to be fully assembled VLPs .

The third population, viral RNAs that appeared at the plasma membrane and remained there for the duration of the observation period (Fig. 3 *A* and *B*), are likely RNA molecules that were recruited to the plasma membrane by Gag. This population was not detected when the packaging-impaired viral RNA was used (Fig. 3*C*, column 5). At the earlier time points, Gag was not

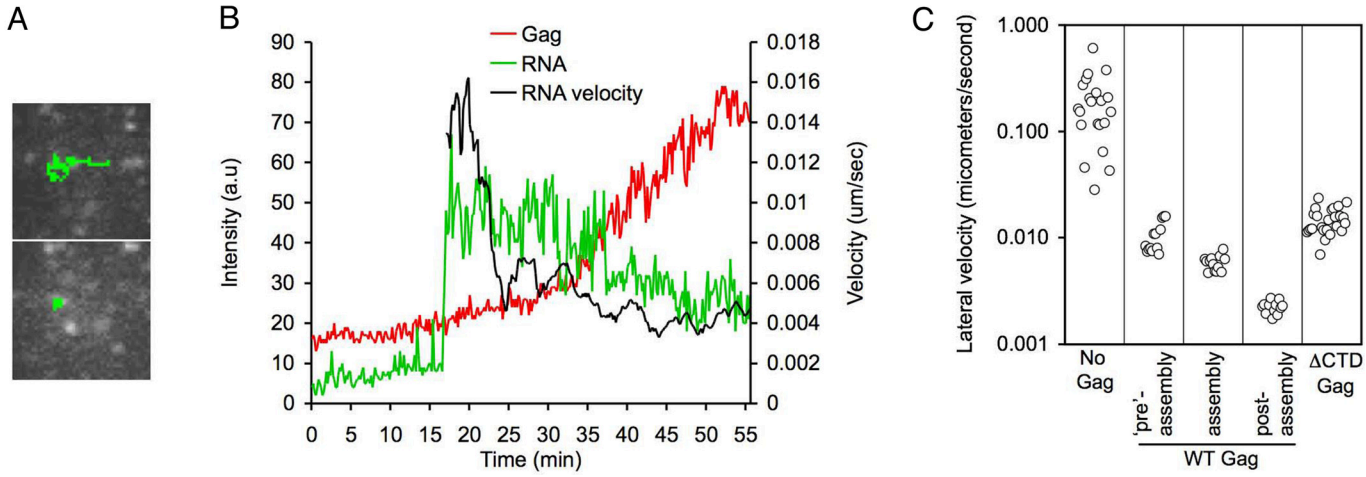

Fig. 4. Lateral movement of HIV-1 genomes in the absence and presence of Gag. (*A*) Images showing the track taken by a GFP-labeled RNA punctum before (top) and after (bottom) the Gag punctum became detectable coincident with the RNA. Images are 5 × 5 μm. (*B*) Plots of fluorescence intensities of Gag and RNA in arbitrary units (a.u), are plotted for the VLP shown in (*A*) Also plotted is the lateral velocity of the RNA, averaged using a sliding window of 21 frames (3.5 min). (*C*) Lateral velocity of RNAs in the TIR field under various conditions. Each point represents the velocity of an individual GFP-labeled RNA punctum. Velocities were averaged over the entire time the RNA molecule was observed in the field in the absence of Gag (No Gag) or in the presence of Gag-ΔCTD. For RNAs anchored at the membrane in the presence of WT Gag, velocities were averaged over (*i*) the time that Gag was undetectable ('pre'-assembly), (*ii*) the time during which Gag fluorescence increased (assembly), and (*iii*) the time during which Gag fluorescent reached a plateau (postassembly). The same thirteen GFP-labeled RNA puncta, from three different cells were evaluated for each phase of assembly.

detectable at the same location as the anchored RNA molecules (Fig. 3 *A* and *B*). A few minutes after appearance of each RNA molecule in the TIR field, Gag began to appear in the same location (mean 4.5 min after the appearance of the RNA, n = 75) (Fig. 3 *A* and *B*). The Gag fluorescence then increased, typically over 5–7 min, and reached a plateau, in the same way that we have previously documented for assembly of VLPs (18). Before the detection of Gag, these RNA molecules moved slowly in the plane of the membrane (≈0.01 μm/s, Fig. 4). However, the increase in Gag fluorescence coincided with decreased lateral velocities of the RNA molecules, culminating in the formation of Gag-positive, RNA-positive puncta, presumably representing assembled VLPs, that were virtually static (Fig. 4). The appearance of each RNA punctum at the plasma membrane was always observed as a single step increase in fluorescence. Once RNA puncta appeared at the plasma membrane, their fluorescence never increased further as Gag accumulated around them or at subsequent time points [(n = 75), see Fig. S8 for examples]. Since complete virions are known to contain dimeric viral genomes, this suggests that the viral genomes are recruited as a preformed dimer, rather than as individual molecules that subsequently dimerize during or after packaging.

While our imaging sensitivity is close to the level of single fluorophores, there is a diffuse level of Gag across the plasma membrane that makes it difficult to resolve whether there are a few Gag molecules specifically associated with the genome when it first reaches the membrane. However, these data suggest a model in which a subdetectable number of Gag molecules are responsible for the initial anchoring of RNA molecules to the plasma membrane.

To test if assembly of Gag was required to anchor viral RNA to the plasma membrane, we generated a Gag protein in which the CTD domain of capsid (Gag-ΔCTD) was deleted. This Gag molecule retains protein domains required for membrane and RNA binding, but lacks Gag-Gag contact sites required for particle assembly. When the Gag-ΔCTD-mCherry protein was expressed in cells, it accumulated at the plasma membrane but its fluorescence remained diffusely distributed at the membrane: no puncta were detected (Fig. S9). In the presence of Gag-ΔCTD-mCherry, GFP-labeled viral genomes became anchored at the plasma membrane (Fig. S10 and Movie S8) but these genomes sometimes dissociated from the plasma membrane, in contrast to molecules anchored by WT Gag (Fig. S10*C*). However, the residence time of Gag-ΔCTD-anchored RNA molecules at the plasma membrane (8.3 min) (Fig. 3*C*, column 5) was significantly longer than the time that would typically elapse between RNA recruitment and the time at which accumulation of larger numbers of WT Gag molecules would become visible (4.5 min). Moreover, 8.3 min may underestimate the residence time of Gag-ΔCTD anchored RNAs because only those that dissociated from the plasma membrane during the observation period (≈50% of the anchored RNA molecules) were used to derive the estimate (Fig. S10*C*).

RNA molecules that were anchored at the plasma membrane by Gag-ΔCTD exhibited slow lateral movement, characteristic of RNA that was anchored by WT Gag during the early phase of assembly (Fig. 4*C* and Movie S8). However, the RNA molecules that were anchored by Gag-ΔCTD never transitioned to moving more slowly. These data confirm that Gag is responsible for RNA anchoring at the plasma membrane, and that Gag molecules that are yet to assemble into VLPs are capable of recruiting viral RNA molecules to the plasma membrane. These data also suggest that at the later stage, RNA movement is reduced as a consequence of the recruitment of additional Gag molecules and, ultimately, the assembly of the virion particle.

The fluorescence of WT Gag-mCherry increased on GFP-labeled viral genomes with the same kinetics that we have previously characterized in the absence of viral RNA (18), Moreover, assembly of Gag-mCherry on HIV-1 RNA puncta represented 75% (n = 100) of all assembly events that occurred in cells where cytoplasmic viral RNA was available. For 15% of assembly events, Gag-mCherry VLPs appeared at locations where no GFP-labeled HIV RNA was detectable. These events could represent assembly on viral RNA that is bound to a low and undetectable number of MS2-GFP molecules, or assembly on cellular RNAs. In the remaining 10% of the cases, the GFP-labeled RNA molecules were detected soon after the detection of puncta of nascent Gag-mCherry VLPs, early during the assembly process.

The fourth population of viral RNA molecules contained both

Gag-mCherry and GFP-labeled RNA and appeared only transiently at the plasma membrane (Fig. S6). These are likely to be VLPs that had been internalized after completion of assembly. We have previously observed a population of VLPs that move rapidly in and out the field adjacent to the plasma membrane and we have demonstrated that these are also labeled with markers for internal endocytic compartments including clathrin and CD63 (18) Several lines of evidence indicate that these endosome-localized particles are not productive preassembly intermediates (15, 16, 28).

Discussion

Based on the observations presented herein, we propose that a small number of Gag molecules bind viral RNA, likely as a preformed dimer, and that this subvirion complex is responsible for anchoring the HIV genome at the plasma membrane. Once anchored, the genome-Gag complex can drift slowly in the plane of the membrane until it nucleates further accumulation of Gag and the subsequent assembly of a complete virion. Recruitment of the viral RNA is reversible if assembly of Gag is disrupted. However, the time typically required for viral RNA to dissociate from an assembly-defective Gag molecule (Gag-ΔCTD) is greater than the time required for WT Gag molecules to accumulate at the site of assembly. Presumably, this second phase of assembly, during which the bulk of Gag recruitment occurs, contributes further RNA anchoring contacts, making genome anchoring and particle assembly effectively irreversible.

The observations described here are not consistent with a number of alternative models for HIV-1 assembly. First, they are not consistent with a model by which multiple genomes and multiple Gag molecules coalesce at the plasma membrane into a single puncta, with assembly driving the elimination of the excess RNA. Second, they are not consistent with a model by which the genome nucleates assembly of Gag in the cytosol before reaching the plasma membrane. Third, they are not consistent with a model in which Gag assembly is substantially completed before the genome is recruited. Rather, the steps in virion genesis described herein that have not previously been observed, lead to a compelling model for genome recruitment and the nucleation of HIV-1 assembly.

In cells where HIV-1 genomic RNA was available for packaging, 75% of the assembly events occurred on an HIV-1 RNA-Gag complex. This finding is consistent with the notion that RNA plays a scaffolding role in assembly, and that HIV-1 genome-Gag complexes at the plasma membrane are highly favored sites for assembly. In 15% of cases, VLPs assembled at locations where no GFP-labeled RNA was detectable. These events could represent assembly on viral RNA that is bound to an undetectable number of MS2-GFP molecules, or assembly on cellular RNAs. In the remaining 10% of the cases, the GFP labeled HIV-1 RNA molecules became detectable as the Gag-mCherry accumulated in VLPs. In these cases, assembly may have initiated on cellular RNAs which were then displaced by viral RNA associated with other Gag molecules that were recruited to those VLPs. Overall, therefore, approximately 85% of the observed VLP assembly events resulted in the encapsidation of viral genomes.

The HIV-1 genomic RNA, unlike cellular RNAs, has specific binding sites for Gag embedded within in the Ψ sequence. This could have led to a faster rate of assembly for VLPs associated with viral RNA than those associated with cellular RNA. However, we did not detect any difference in the assembly times of VLPs in the presence of absence of the HIV-1 genome (mean 9.09 min, SD 3.54, $n = 25$ vs. 8.11 min, SD 2.21, $n = 25$, respectively). A caveat to this conclusion is that our measurements of Gag assembly times only document the time period between the first detectable Gag and the completion of assembly. Indeed, the ability to monitor the arrival of the viral RNA allows us to measure an additional, previously unobserved parameter in HIV-1 assembly. Specifically, following detection of the anchored HIV-1 genome at the plasma membrane, approximately 4–5 min typically elapsed before detectable levels of Gag accumulated on this Gag-RNA subvirion complex. The nature of the RNA (cellular or viral) in the initial Gag-RNA complex may affect the very early kinetics, for example the recruitment of the second, third, or fourth molecules of Gag to the initial Gag-RNA complex. Nonetheless, once a critical number of Gag molecules at the site of assembly is reached (that correlates with our ability to detect a nascent Gag punctum) subsequent Gag recruitment, and the time to complete assembly appears to be independent of the presence of the HIV-1-specific versus cellular RNA. This makes sense, given that there are only a few specific binding sites for HIV-1 Gag in the Ψ sequence of the HIV-1 genome, and several thousand molecules of Gag in the complete virion (29) Clearly, the vast majority of the Gag molecules in a complete virion must be associated with the HIV-1 genome in an RNA sequence-independent manner. Thus, our data suggest a model in which the complex that initially anchors RNA to the plasma membrane includes one or a few molecules of Gag bound to Ψ, while subsequent Gag recruitment involves specific Gag-Gag interactions and non-specific Gag-RNA interactions. This second phase of assembly would predictably occur with equal efficiency irrespective of the identity of the packaged RNA.

While these studies have allowed us to identify previously unobserved intermediates in the assembly of the HIV-1 virion, they do not determine the subcellular location of the initial genome recognition by Gag. Gag and RNA could interact before membrane association and then move to assembly sites as a subcomplex; alternatively they could reach the plasma membrane independently, where they would subsequently interact. We show here that the anchoring of the HIV-1 RNA to the plasma membrane is due to interactions with Gag molecules that are, for now, too few in number for us to detect, but likely fewer than 12 Gag molecules based on our sensitivity of detection. This emphasizes the difficulties in resolving the initial site of recognition between Gag and RNA.

We note that MLV RNA has been reported to traffic with Gag within endosomes in a microtubule-dependent fashion and proposed to travel in this way to viral assembly sites (30). However, in that study, which was performed using cells stably expressing MLV Gag, the RNA-Gag complexes may represent fully formed virions that have been endocytosed subsequent to assembly. In fact, fully assembled MLV and HIV-1 particles are internalized into CD63-positive endosomes after completion of assembly at the plasma membrane (15, 18, 28). These endocytosed VLPs exhibit highly dynamic movements reminiscent of microtubule-based transport (18). Therefore, further studies are warranted to determine where in the cell RNA is first recognized by Gag.

The mechanisms that drive HIV-1 RNA movement through the cytoplasm are poorly understood. Two mechanisms for cytoplasmic transport of cellular mRNAs have been reported: diffusion followed by local trapping and active transport along the cytoskeleton (31). Our observations of HIV-1 RNA, and the apparent absence of directed movement, tentatively suggest that the diffusion/trapping model may be operative during the genesis of HIV-1 particles. However, the methods developed here provide appropriate tools to explore the mechanisms that govern the transport of HIV-1 genomic RNA throughout the cell.

Materials and Methods

Plasmid Derivation. Plasmids for the expression of HIV-1 Gag or MS2-GFP fusion proteins or the MS2-tagged HIV-1 genome were described previously (18, 21, 32), or are described in the *SI Methods*.

Cells, Transfection, and Infection. A HeLa cell line stably expressing MS2-NLS-GFP was generated as described in the *SI Methods*. 293T cells were transfected using polyethylenimine (PolySciences), and HeLa cells were transfected using Lipofectamine 2000 (Invitrogen). Infectivity assays were carried out using virons generated in 293T cells as described in the *SI Methods*

Image Acquisition and Analysis. For microscopic analysis, VLPs (generated as described in the *SI Methods*) or HeLa cells were plated on glass-bottomed dishes (MatTek). Cells were transfected with an excess of an untagged version of Gag (the ratio of Gag-mCherry to untagged Gag was 1:5) to avoid the morphological defect of particles assembled from fluorescent Gag only (33). Cells were transfected with a total of 2 μg DNA (1 μg Gag/Gag-mCherry and 1 μg RNA reporter plasmids).

For epifluorescence microscopy, cells were fixed 18–20 h after transfection and nuclei were stained with Hoechst 33258, as previously described (28). Fluorescent imaging of fixed cells was done using an Deltavision microscopy suite, as previously described (28). For live cell TIR-FM, cells were imaged 5–8 h after transfection, without fixation, as described in the *SI Methods*. The camera and shutters were controlled using MetaMorph software (Molecular Devices). Time-lapse movies were acquired over a 10- to 60-min period with one image acquired every 5 or 10 s. Alternatively, for imaging HIV-1 RNA alone, the 'stream' mode of acquisition was used with images acquired at 3–5 frames/s for 10–15 s.

All data analyses used MetaMorph software. For dual-color movie sequences, the images acquired through the emission splitter were separated, aligned with an accuracy of a single pixel, and analyzed. For measuring the intensity of fluorescent puncta, a region was drawn around an area of interest of 10 $\times$ 10 pixels and the maximum intensity within this region recorded. For tracking VLPs and RNA over time, the 'tracking object' option of the software was used. This option allowed the calculation of velocities. The time to complete assembly was defined as the elapsed time from the image at which a fluorescent Gag signal is first detectable to the point when Gag intensity reaches a plateau.

ACKNOWLEDGMENTS. We thank Robert Singer (Albert Einstein College of Medicine) for the MS2 reagents. This work was supported by a Foundation for AIDS Research postdoctoral fellowship (to N.J.), National Institutes of Health Grant R01AI50111 (to P.D.B.), and National Science Foundation Grants BES-0620813 and BES-0322867 (to S.M.S.). P.D.B. is a Howard Hughes Medical Institute investigator.

1. Ganser-Pornillos BK, Yeager M, Sundquist WI (2008) The structural biology of HIV assembly. *Curr Opin Struct Biol* 18:203–217.
2. Bieniasz PD (2009) The cell biology of HIV-1 virion genesis. *Cell Host Microbe* 5:550–558.
3. D'Souza V, Summers MF (2005) How retroviruses select their genomes. *Nat Rev Microbiol* 3:643–655.
4. Lever A, Gottlinger H, Haseltine W, Sodroski J (1989) Identification of a sequence required for efficient packaging of human immunodeficiency virus type 1 RNA into virions. *J Virol* 63:4085–4087.
5. Harrison GP, Lever AM (1992) The human immunodeficiency virus type 1 packaging signal and major splice donor region have a conserved stable secondary structure. *J Virol* 66:4144–4153.
6. Luban J, Goff SP (1994) Mutational analysis of cis-acting packaging signals in human immunodeficiency virus type 1 RNA. *J Virol* 68:3784–3793.
7. Clever J, Sassetti C, Parslow TG (1995) RNA secondary structure and binding sites for gag gene products in the 5′ packaging signal of human immunodeficiency virus type 1. *J Virol* 69:2101–2109.
8. Clever JL, Wong ML, Parslow TG (1996) Requirements for kissing-loop-mediated dimerization of human immunodeficiency virus. RNA *J Virol* 70:5902–5908.
9. Skripkin E, Paillart JC, Marquet R, Ehresmann B, Ehresmann C (1994) Identification of the primary site of the human immunodeficiency virus type 1 RNA dimerization in vitro. *Proc Natl Acad Sci USA* 91:4945–4949.
10. Amarasinghe GK, De Guzman RN, Turner RB, Chancellor KJ, Wu ZR, Summers MF (2000) NMR structure of the HIV-1 nucleocapsid protein bound to stem-loop SL2 of the psi-RNA packaging signal. Implications for genome recognition. *J Mol Biol* 301:491–511.
11. De Guzman RN, Wu ZR, Stalling CC, Pappalardo L, Borer PN, Summers MF (1998) Structure of the HIV-1 nucleocapsid protein bound to the SL3 psi-RNA recognition element. *Science* 279:384–388.
12. Rulli SJ, Jr, Hibbert CS, Mirro J, Pederson T, Biswal S, Rein A (2007) Selective and nonselective packaging of cellular RNAs in retrovirus particles. *J Virol* 81:6623–6631.
13. Muriaux D, Mirro J, Harvin D, Rein A (2001) RNA is a structural element in retrovirus particles. *Proc Natl Acad Sci USA* 98:5246–5251.
14. Campbell S, Vogt VM (1995) Self-assembly in vitro of purified CA-NC proteins from Rous sarcoma virus and human immunodeficiency virus type 1. *J Virol* 69:6487–6497.
15. Jouvenet N, et al. (2006) Plasma membrane is the site of productive HIV-1 particle assembly. *PLoS Biol* 4:e435.
16. Finzi A, Orthwein A, Mercier J, Cohen EA (2007) Productive human immunodeficiency virus type 1 assembly takes place at the plasma membrane. *J Virol* 81:7476–7490.
17. Welsch S, Keppler OT, Habermann A, Allespach I, Krijnse-Locker J, Krausslich HG (2007) HIV-1 buds predominantly at the plasma membrane of primary human macrophages. *PLoS Pathog* 3:e36.
18. Jouvenet N, Bieniasz PD, Simon SM (2008) Imaging the biogenesis of individual HIV-1 virions in live cells. *Nature* 454:236–240.
19. Fusco D, et al. (2003) Single mRNA molecules demonstrate probabilistic movement in living mammalian cells. *Curr Biol* 13:161–167.
20. Bertrand E, Chartrand P, Schaefer M, Shenoy SM, Singer RH, Long RM (1998) Localization of ASH1 mRNA particles in living yeast. *Mol Cell* 2:437–445.
21. Zennou V, Perez-Caballero D, Gottlinger H, Bieniasz PD (2004) APOBEC3G incorporation into human immunodeficiency virus type 1 particles. *J Virol* 78:12058–12061.
22. Cullen BR (2003) Nuclear mRNA export: Insights from virology. *Trends Biochem Sci* 28:419–424.
23. Amarasinghe GK, De Guzman RN, Turner RB, Summers MF (2000) NMR structure of stem-loop SL2 of the HIV-1 psi RNA packaging signal reveals a novel A-U-A base-triple platform. *J Mol Biol* 299:145–156.
24. Valegard K, Murray JB, Stockley PG, Stonehouse NJ, Liljas L (1994) Crystal structure of an RNA bacteriophage coat protein-operator complex. *Nature* 371:623–626.
25. Gottlinger HG, Sodroski JG, Haseltine WA (1989) Role of capsid precursor processing and myristoylation in morphogenesis and infectivity of human immunodeficiency virus type 1. *Proc Natl Acad Sci USA* 86:5781–5785.
26. Bryant M, Ratner L (1990) Myristoylation-dependent replication and assembly of human immunodeficiency virus 1. *Proc Natl Acad Sci USA* 87:523–527.
27. Neil SJ, Zang T, Bieniasz PD (2008) Tetherin inhibits retrovirus release and is antagonized by HIV-1 Vpu. *Nature* 451:425–430.
28. Neil SJ, Eastman SW, Jouvenet N, Bieniasz PD (2006) HIV-1 Vpu promotes release and prevents endocytosis of nascent retrovirus particles from the plasma membrane. *PLoS Pathog* 2:e39.
29. Briggs JA, et al. (2004) The stoichiometry of Gag protein in HIV-1. *Nat Struct Mol Biol* 11:672–675.
30. Basyuk E, Galli T, Mougel M, Blanchard JM, Sitbon M, Bertrand E (2003) Retroviral genomic RNAs are transported to the plasma membrane by endosomal vesicles. *Dev Cell* 5:161–174.
31. St Johnston D (2005) Moving messages: The intracellular localization of mRNAs. *Nat Rev Mol Cell Biol* 6:363–375.
32. Perez-Caballero D, Hatziioannou T, Martin-Serrano J, Bieniasz PD (2004) Human immunodeficiency virus type 1 matrix inhibits and confers cooperativity on gag precursor-membrane interactions. *J Virol* 78:9560–9563.
33. Larson DR, Johnson MC, Webb WW, Vogt VM (2005) Visualization of retrovirus budding with correlated light and electron microscopy. *Proc Natl Acad Sci USA* 102:15453–15458.